

Molecular Gradients: An Efficient Approach for Optimizing the Surface Properties of Biomaterials and Biochips

Michael Riepl,^{†,‡} Mattias Östblom,[†] Ingemar Lundström,[§] Stefan C. T. Svensson,^{||} Arnoud W. Denier van der Gon,^{⊥,○} Michael Schäferling,^{†,‡} and Bo Liedberg^{*,†}

Divisions of Sensor Science and Molecular Physics, Applied Physics, Chemistry, and Surface Physics and Chemistry, Department of Physics and Measurement Technology, Linköping University, SE-58183 Linköping, Sweden

Received July 2, 2004. In Final Form: November 9, 2004

A variety of molecular gradients of alkanethiols with the structure HS-(CH₂)_m-X (*m* = 15; X = COOH, CH₂NH₂, or CH₃) and oligo(ethylene glycol)-terminated alkanethiols with the structures HS-(CH₂)₁₅-CO-NH-Eg_{*n*} (*n* = 2, 4, or 6), HS-(CH₂)₁₅-CO-NH-Eg₂-(CH₂)₂-NH-CO-(CH₂)₄-biotin, and HS-(CH₂)₁₅-CO-NH-Eg₆-CH₂-COOH were prepared on polycrystalline gold films. These gradients were designed to serve as model surfaces for fundamental studies of protein adsorption and immobilization phenomena. Ellipsometry, infrared spectroscopy, and X-ray photoelectron spectroscopy, operating in scanning mode, were used to monitor the layer composition, gradient profiles, tail group conformation, and overall structural quality of the gradient assemblies. The gradient profiles were found to be 4–10 nm wide, and they increased in width with increasing difference in molecular complexity between the thiols used to form the gradient. The oligo(ethylene glycol) thiols are particularly interesting because they can be used to prepare so-called conformational gradients, that is, gradients that display a variation in oligo(ethylene glycol) chain conformation from *all-trans* on the extreme Eg_{2,4} sides, via an *amorphous*-like phase in the mixing regimes, to *helical* at the extreme Eg₆ sides. We demonstrate herein a series of experiments where the above gradients are used to evaluate nonspecific binding of the plasma protein fibrinogen, and in agreement with previous studies, the highest amounts of nonspecifically bound fibrinogen were observed on *all-trans* monolayers, that is, on the extreme Eg_{2,4} sides. Moreover, gradients between Eg₂ and a biotinylated analogue have been prepared to optimize the conditions for the immobilization of streptavidin. Ellipsometry and infrared spectroscopy reveal high levels of immobilization over a fairly broad range of compositions in the gradient regime, with a maximum between 50 and 60% of the biotinylated analogue in the monolayer. A pl gradient composed of (NH₃⁺/COO⁻)-terminated thiols was also prepared and evaluated with respect to its ability to separate differently charged proteins, pepsin, and lysozyme, on a solid surface.

Introduction

Self-assembled monolayers (SAMs) of *ω*-substituted alkanethiols and disulfides on gold have been thoroughly studied since the early 1980s.^{1–5} Alkanethiol SAMs on gold are well organized, densely packed, and very stable against chemical and mechanical stress. They have therefore found applications in many technological areas, such as micro- and nanoscale patterning,^{6–8} molecular electronics,^{9,10} and (bio)chemical sensing.^{11–14} In particular, the ability to form mixed monolayers from binary mixtures of *ω*-functionalized alkanethiols (HS-(CH₂)_{*n*}-

X)/(HS-(CH₂)_{*m*}-Y) has attracted interest from several research groups,^{15–20} because it allows excellent control of the surface properties on a molecular level by using different tail groups, chain lengths, spacers, and solvents.

* Corresponding author. Phone: +46-13-281877. Fax: +46-13-288969. E-mail: bol@ifm.liu.se.

[†] Division of Sensor Science and Molecular Physics.

[‡] Present address: Advalytix AG, Eugen-Sänger-Ring 4, D-85649 Brunthal-Nord, Germany.

[§] Division of Applied Physics.

^{||} Division of Chemistry.

[⊥] Division of Surface Physics and Chemistry.

[○] On leave from the Faculty of Applied Physics, Eindhoven University of Technology, 5600 MB Eindhoven, The Netherlands. Deceased, 2003.

[#] Present address: Institute for Analytical Chemistry, University of Regensburg, D-93040 Regensburg, Germany.

(1) Nuzzo, R. G.; Allara, D. L. *J. Am. Chem. Soc.* **1983**, *105*, 4481–4483.

(2) Porter, M. D.; Bright, T. B.; Allara, D. L.; Chidsey, C. E. D. *J. Am. Chem. Soc.* **1987**, *109*, 3559–3568.

(3) Ulman, A. *An Introduction to Ultrathin Organic Films: From Langmuir Blodgett to Self-Assembly*; Academic Press: New York, 1991.

(4) Ulman, A. *Chem. Rev.* **1996**, *96*, 1533–1554.

(5) Schreiber, F. *Prog. Surf. Sci.* **2000**, *65*, 151–256.

(6) Xia, Y.; Whitesides, G. M. *Angew. Chem., Int. Ed.* **1998**, *37*, 550–575.

(7) Jackman, R. J.; Wilbur, J. L.; Whitesides, G. M. *Science* **1995**, *269*, 664–666.

(8) Mrkisch, M.; Chen, C. S.; Xia, Y.; Dike, L. E.; Inber, D. E.; Whitesides, G. M. *Proc. Natl. Acad. Sci. U.S.A.* **1996**, *93*, 10775–10778.

(9) Bumm, L. A.; Arnold, J. J.; Cygan, M. T.; Dunbar, T. D.; Burgin, T. P.; Jones, L.; Allara, D. L.; Tour, J. M.; Weiss, P. S. *Science* **1996**, *271*, 1705–1707.

(10) Cai, L. T.; Skulason, H.; Kushmerick, J. J.; Pollack, S. K.; Naciri, J.; Shashidhar, R.; Allara, D. L.; Mallouk, T. E.; Mayer, T. S. *J. Phys. Chem.* **2004**, *108*, 2827–2832.

(11) Spinke, J.; Liley, M.; Guder, H.-J.; Angermaier, L.; Knoll, W. *Langmuir* **1993**, *9*, 1821–1825.

(12) Lahiri, J.; Isaacs, L.; Tien, J.; Whitesides, G. M. *Anal. Chem.* **1999**, *71*, 777–790.

(13) Svedhem, S.; Öhberg, L.; Borrelli, S.; Valiokas, R.; Andersson, M.; Oscarsson, S.; Svensson, S. C. T.; Liedberg, B.; Koradsson, P. *Langmuir* **2002**, *18* (7), 2848–2858.

(14) Schäferling, M.; Riepl, M.; Pavlickova, P.; Kambhampati, D.; Liedberg, B. *Microchim. Acta* **2003**, *142*, 193–203.

(15) Folkers, J. P.; Laibinis, P. E.; Whitesides, G. M. *Langmuir* **1992**, *8*, 1330–1341.

(16) Laibinis, P. E.; Nuzzo, R. G.; Whitesides, G. M. *J. Phys. Chem.* **1992**, *96*, 5097–5105.

(17) Bertilsson, L.; Liedberg, B. *Langmuir* **1993**, *9*, 141–149.

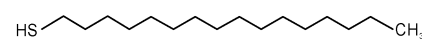
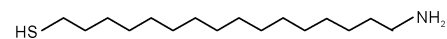
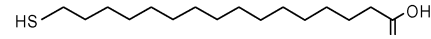
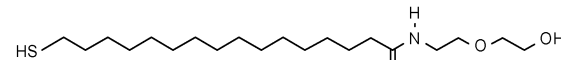
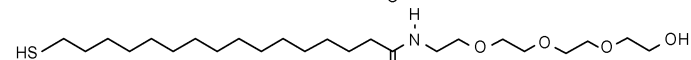
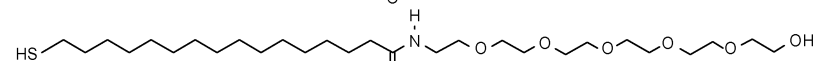
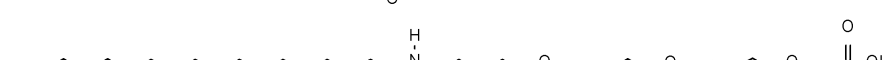
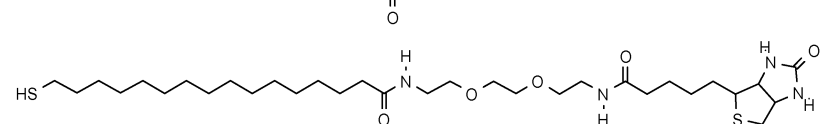
(18) Folkers, J. P.; Laibinis, P. E.; Whitesides, G. M.; Deutch, J. J. *Phys. Chem.* **1994**, *98*, 563–571.

(19) Stranick, S. J.; Parikh, A. N.; Tao, Y.-T.; Allara, D. L.; Weiss, P. S. *J. Phys. Chem.* **1994**, *98*, 7636–7646.

(20) Yang, Z.; Engquist, I.; Wirde, M.; Kauffmann, J.-M.; Gelius, U.; Liedberg, B. *Langmuir* **1997**, *13*, 3210–3218.

Chart 1

Structure of the molecule

	Abbreviation	Thickness, nm
	C ₁₅ -CH ₃	2.15
	C ₁₆ -NH ₂	2.35
	C ₁₅ -COOH	2.20
	Eg2	2.80
	Eg4	3.35
	Eg6	3.85
	Eg6-COOH	4.30
	Biotin-OEG	3.90

Another way to create mixed monolayers is to use the molecular gradient approach developed at our laboratory.²¹ The advantage of the gradient approach is that one can introduce a continuously varying chemical composition profile from 100% of X to 100% of Y (see above) on a single substrate surface. Early studies from our group on this topic focused on structural investigations of gradients prepared using long-chain alkanethiols having relatively simple tail groups.^{21–23} The objective of the present contribution is (I) to describe the preparation and characterization of more complex gradients and (II) to demonstrate how they can be applied to address critical issues regarding specific as well as nonspecific interaction and adsorption phenomena occurring at biosensing and biomaterial surfaces.

The gradient approach in itself is not entirely new to the biomaterials and sensing communities. Elwing and Gölander, for example, generated analogous gradients based on organosilanes and silica, in particular hydrophobicity gradients, for protein exchange and biomaterials applications.^{24–26} Corona discharge techniques also have been used to prepare hydrophobicity gradients on polymers.^{27,28} Wu et al. prepared grafting density gradients of poly(acrylamide) on a silica surface and used wettability experiments to gain information about the nature of a mushroom-to-brush transition.²⁹ Venkateswar et al. utilized an electrophoretic method in combination with microstamping to generate biomolecule gradients.³⁰ More recently, Bohn et al. utilized electrochemical methods to generate peptide-alkanethiol and nanosphere gradients on metals.^{31–33} Microscale protein gradients have also been prepared using heterobifunctional photolinkers containing benzophenone.³⁴ It also should be emphasized that diffusion-controlled gas phase silanization of silica has been utilized to prepare hydrophobicity gradients for applications outside the biomaterial and bioanalytical communities.^{35,36} Platinum catalyst gradients also have been generated and studied with scanning electrochemical microscopy.³⁷

Oligo(ethylene glycol) (OEG)-terminated alkanethiols are very interesting compounds that can be used to form

SAMs with tailored properties.^{38–42} They are well-known to reduce nonspecific adsorption of proteins and appear therefore to be good candidates for certain biomaterials^{43,44} and biosensing applications.^{13,45} The structural properties

- (21) Liedberg, B.; Tengvall, P. *Langmuir* **1995**, *11*, 3821–3827.
 (22) Liedberg, B.; Wirde, M.; Tao, Y.-T.; Tengvall, P.; Gelius, U. *Langmuir* **1997**, *13*, 5329–5334.
 (23) Welin-Klintström, S.; Lestelius, M.; Liedberg, B.; Tengvall, P. *Colloids Surf., B* **1999**, *15*, 81.
 (24) Elwing, H.; Gölander, C.-G. *Adv. Colloid Interface Sci.* **1990**, *32*, 317–339.
 (25) Welin-Klintström, S.; Askendahl, A.; Elwing, H. *J. Colloid Interface Sci.* **1993**, *158*, 188–194.
 (26) Lin, Y. S.; Hlady, V.; Gölander, C.-G. *Colloids Surf., B* **1994**, *3*, 49–62.
 (27) Pitt, W. G. *J. Colloid Interface Sci.* **1989**, *133*, 223–227.
 (28) Lee, L. H.; Lee, H. B. *J. Biomater. Sci., Polym. Ed.* **1993**, *4*, 467–481.
 (29) Venkateswar, R. A.; Branch, D. W.; Wheeler, B. C. *Biomed. Microdevices* **2000**, *2*, 255–264.
 (30) Wu, T.; Efimenko, K.; Vlček, P.; Šubr, V.; Genzer, J. *Macromolecules* **2003**, *36*, 2448–2453.
 (31) Wang, Q.; Bohn, P. W. *J. Phys. Chem.* **2003**, *107*, 12578–12584.
 (32) Wang, Q.; Jakubowski, J. A.; Sweedler, J. V.; Bohn, P. W. *Anal. Chem.* **2004**, *76*, 1–8.
 (33) Plummer, S. T.; Bohn, P. W. *Langmuir* **2002**, *18*, 4142–4149.
 (34) Hypolite, C. L.; McLernon, T. L.; Adams, D. N.; Chapman, K. E.; Herbert, C. B.; Huang, C. C.; Distefano, M. D.; Hu, W.-S. *Bioconjugate Chem.* **1997**, *8*, 658–663.
 (35) Chaudhury, M. K.; Whitesides, G. M. *Science* **1992**, *256*, 1539–1541.
 (36) Daniel, S.; Chaudhury, M. K.; Chen, J. C. *Science* **2001**, *291*, 633–636.
 (37) Jayaraman, S.; Hillier, A. C. *Langmuir* **2001**, *17*, 7857–7864.
 (38) Pale-Grosdemange, C.; Simon, E. S.; Prime, K. L.; Whitesides, G. M. *J. Am. Chem. Soc.* **1991**, *113*, 12–20.
 (39) Prime, K. L.; Whitesides, G. M. *Science* **1991**, *252*, 1164–1167.
 (40) Harder, P.; Grunze, M.; Dahint, R.; Whitesides, G. M.; Laibinis, P. E. *J. Phys. Chem.* **1998**, *102*, 426–436.
 (41) Vanderah, D. J.; Meuse, D. J.; Silin, C. W.; Plant, A. *Langmuir* **1998**, *14*, 6916–6923.
 (42) Valiokas, R.; Svedhem, S.; Svensson, S. C. T.; Liedberg, B. *Langmuir* **1999**, *15*, 3390–3394.
 (43) Benesh, J.; Svedhem, S.; Svensson, S. C. T.; Valiokas, R.; Liedberg, B.; Tengvall, P. *J. Biomater. Sci., Polym. Ed.* **2001**, *12*, 581–597.
 (44) Schwendel, D.; Dahint, R.; Herrwerth, S.; Schloerholtz, M.; Eck, W.; Grunze, M. *Langmuir* **2001**, *17*, 5717–5720.
 (45) Riepl, M.; Schäferling, M.; Kuschina, M.; Ortigao, F.; Liedberg, B. *Langmuir* **2002**, *18*, 7016–7023.

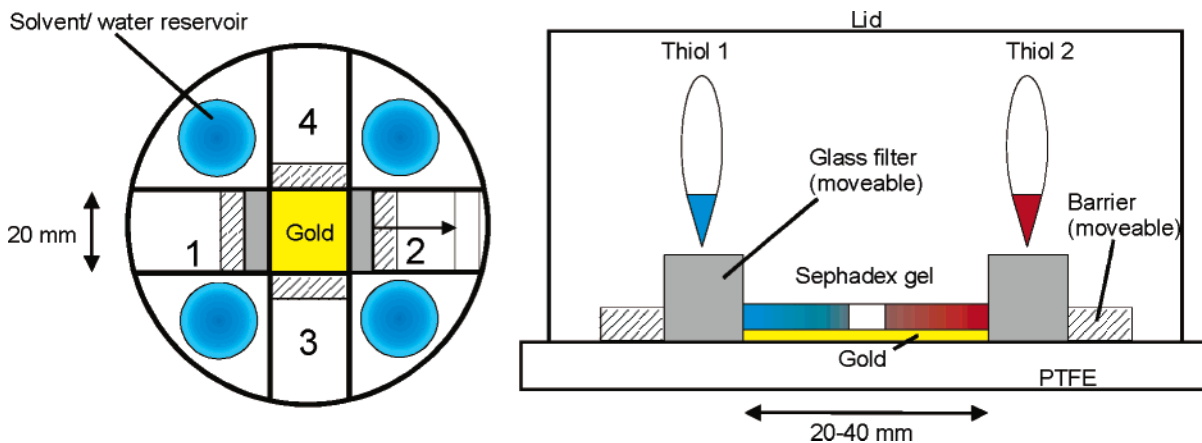


Figure 1. Schematic drawing of the top (left) and the side (right) views of the cross-diffusion geometry used for the preparation of the molecular gradients. The movable barriers, seen in tracks 1 and 2, are inserted to regulate the diffusion of the molecules in one direction. The setup was covered with a lid to keep the experimental conditions (e.g., humidity) constant during the diffusion process, 24–48 h.

of OEG monolayers^{46–49} as well as their functional properties in contact with various fluids have been studied in detail by several groups.^{50,51} Modification of the head-group from hydroxyl to biotin or carboxyl offers the possibility to anchor a broad spectrum of biomolecules to an OEG SAM.^{14,45} In this study, we report on the characterization of a series of gradients, primarily those containing OEG tails with different tail groups of the general structure HS-(CH₂)₁₅-CO-NH-Eg_n-X (*n* = 2, 4, or 6), Chart 1, using scanning infrared (IR) spectroscopy, X-ray photoelectron spectroscopy (XPS), and null ellipsometry. Proteins such as fibrinogen and streptavidin were subsequently exposed to the gradients in an attempt to improve the understanding of the monolayer properties leading to low levels of nonspecific adsorption and to optimize the conditions for the immobilization of streptavidin onto biotinylated surfaces. A pI gradient based on (C₁₆-NH₂/C₁₅-COOH) thiols also has been generated and tested with respect to its ability to separate proteins on a surface, and a proof of concept demonstration using pepsin and lysozyme as model proteins is described. The approach used to prepare 1D gradients from two thiols can easily be extended into 2D using four different thiols, and such studies are currently undertaken at our laboratory.

It should be emphasized that the philosophy of the present contribution is to demonstrate the power of the gradient approach for a range of applications of relevance for the design and development of novel biosensing and biomaterials surfaces. More detailed studies on selected topics will be published separately.

Experimental Section

Materials. The HS-(CH₂)₁₅-CH₃(C₁₅-CH₃) alkanethiol was obtained from Fluka, and the HS-(CH₂)₁₅-COOH(C₁₅-COOH) one was obtained from Prof. D. L. Allara, Penn State University, PA. The oligo(ethylene glycol)-terminated alkanethiols (Eg₂, Eg₄,

Eg₆, and Eg₆-COOH), Chart 1, were synthesized according to previously described methods.⁵² The synthesis of *N*-(8-biotinyl-3,6-dioxaoctanamidyl)-16-mercaptohexadecane-amide (biotin-OEG) has been described elsewhere.⁴⁵ The amino-terminated thiol HS-(CH₂)₁₆-NH₂(C₁₆-NH₂) was obtained from Dr. Johan Ekeröth, Division of Chemistry. The thiols were dissolved in 99.5% ethanol (Kemetyl, Haninge, Sweden.). Streptavidin, fibrinogen, pepsin, and lysozyme were purchased from Sigma.

Sample Preparation. Gold substrates were prepared according to previously described protocols.³⁷ In brief, gold films 200 nm thick were prepared on precut silicon (100) wafers primed with a thin (~2 nm) titanium adhesion layer using a Balzer UMS 500P electron beam evaporation system, operating at an evaporation rate of 0.1 and 1 nm/s for titanium and gold, respectively. The base pressure was kept on the low 10⁻⁹ mbar scale, and the evaporation pressure never exceeded 10⁻⁷ mbar. The gold surfaces were cleaned prior to monolayer and gradient formation in a standard solution (TL1) containing a 5:1:1 mixture of Milli-Q water, 25% hydrogen peroxide, and 30% ammonia for 10 min at 85°C, rinsed carefully in Milli-Q water, and finally blown dry in nitrogen.

Preparation of Gradients. The freshly cleaned gold substrates were immediately used to prepare the gradients using a “cross-diffusion” methodology.²¹ In brief, a clean and bare gold sample, size 2 × 2 cm², was placed in the cross-diffusion cell made of poly(tetrafluoroethylene) (PTFE). The setup, which allows for the preparation of both 1D and 2D gradients, is schematically outlined in Figure 1. The diffusion matrix was prepared by mixing 1 g of Sephadex LH-20 and 5 g of ethanol. A few drops of Millipore water were added to improve the swelling. After 15 min of swelling, it was spread and homogenized on top of the gold slide, and excess ethanol was allowed to evaporate to achieve a constant weight of the matrix. Glass filters with an average pore size of ~100 μm were inserted and used as reservoirs and starting points for the thiol solutions. The concentration of the thiols injected into the glass filters was 1 mM in ethanol, and the diffusion experiments were undertaken at room temperature. The geometry of the cell, Figure 1, forced the thiol molecules to move in a predefined direction along tracks 1–4. This setup is different in regard to our previous setup²¹ because it has PTFE barriers that prevent back-diffusion of the thiol solutions. The barriers are flexible to allow for different sample sizes and diffusion lengths, see arrow track 2. The diffusion time for the formation of the gradients varied between 24 and 48 h, depending on the size, complexity, and retention time of the thiols in the Sephadex matrix. The gradient samples were then removed from the setup and rinsed thoroughly in ethanol, ultrasonicated in ethanol for 5 min, and then rinsed again in ethanol to remove excess physisorbed Sephadex LH20. The samples were finally blown dry in a stream of nitrogen and immediately characterized

(46) Valiokas, R.; Svedhem, S.; Östblom, M.; Svensson, S. C. T.; Liedberg, B. *J. Phys. Chem. B* **2001**, *105*, 5459–5469.

(47) Valiokas, R.; Östblom, M.; Svedhem, S.; Svensson, S. C. T.; Liedberg, B. *J. Phys. Chem. B* **2002**, *106*, 10401–10409.

(48) Wang, R. L. C.; Kreuzer, H. J.; Grunze, M. *J. Phys. Chem. B* **1997**, *101*, 9767–9773. Herrwerth, S.; Eck, W.; Reinhardt, S.; Grunze, M. *J. Am. Chem. Soc.* **2003**, *125*, 9359–9366.

(49) Malysheva, L.; Klymenko, Y.; Onipko, A.; Valiokas, R.; Liedberg, B. *Chem. Phys. Lett.* **2003**, *370*, 451–459.

(50) Zolk, M.; Eisert, F.; Pipper, J.; Herrwerth, S.; Eck, W.; Buck, M.; Grunze, M. *Langmuir* **2000**, *16*, 5849–5852.

(51) Dicke, Ch.; Hähner, G. *J. Am. Chem. Soc.* **2002**, *124*, 12619–12625.

(52) Svedhem, S.; Hollander, C.-Å.; Shi, J.; Konradsson, P.; Liedberg, B.; Svensson, S. C. T. *J. Org. Chem.* **2001**, *66*, 4494–4503.

or immersed into the appropriate protein solution. It should be pointed out that the thiols were injected sequentially and manually into the glass filters, Figure 1. This procedure introduced an uncertainty in the definition of the *absolute* starting point of the gradients. Thus, it is necessary to characterize every sample to obtain the gradient profile, that is, the relation between the composition and the position on the surface. This gradient profile will serve as a reference during subsequent evaluation of the protein adsorption and immobilization profiles. Single component SAMs (for reference purposes, Chart 1) were prepared by immersing gold films into ethanolic solutions containing 100 μ M alkanethiol for 16 h, at room temperature.

Protein Adsorption. The gradients were incubated for 1.5 h at room temperature in protein solutions containing either 250 μ g/mL fibrinogen at pH 6.0, 100 μ g/mL streptavidin at pH 7.4, or 1 mg/mL pepsin and lysozyme at pH 6 (100 mM KCl and 5 mM Na-phosphate). The samples were rinsed carefully with Millipore water and dried before further investigations.

Ellipsometry. The ellipsometric measurements were performed with an automatic Rudolph Research AutoEl III ellipsometer aligned at an angle of incidence of 70° with respect to the surface normal. The ellipsometer was equipped with a He-Ne laser ($\lambda = 632.8$ nm) light source. A model based on isotropic optical constants for the organic (protein) layer, $N_{\text{layer}} = n + ik = 1.50 + i0$, where n represents the refractive index and k the extinction coefficient, was used for the reevaluation of the thicknesses of the SAMs and protein layers. The sample was mounted on a scanning table, and the thickness was measured over the whole length of the gradient, using a step size of 1 mm.

Infrared Measurements. The infrared reflection-absorption (RA) spectra of the single component monolayers were recorded at room temperature on a Bruker IFS 66 system equipped with a grazing angle RA accessory (85°) and a liquid-nitrogen-cooled mercury cadmium telluride (MCT) detector. The acquisition time was around 10 min at 2 cm^{-1} resolution. A three-term Blackman-Harris apodization function was applied to the interferograms before Fourier transformation. An ultrahigh vacuum (UHV) system was used to obtain RA spectra of the gradient samples. This system has been described elsewhere.⁵³ A new spectrum was obtained every 0.5 or 1 mm. The ellipsometry and IR scanning apparatuses utilizes different spot sizes, ~ 1 mm for ellipsometry and ~ 4 mm for IR. Thus, we can in most cases analyze the entire gold surface (gradient profile) with ellipsometry but not with IR because the IR beam will hit the sample holder and/or uncoated areas of the supporting silicon wafer when one approaches the edges of the sample. This reduces generally the number of data points in the IR plots of the gradient profiles as compared to the profiles obtained using ellipsometry.

X-ray Photoelectron Spectroscopy. The XPS spectra of the $\text{C}_{15}\text{COOH}/\text{C}_{15}\text{CH}_3$ gradients were recorded, at a step size of 0.1 mm, using a Scienta ESCA200 spectrometer operating at a base pressure of 2×10^{-10} mbar and with monochromatic Al K α radiation at $h\nu = 1486.7$ eV. The binding energy of the gold $4f_{7/2}$ line was calibrated to 83.9 eV. The experimental conditions were chosen to give a lateral resolution of 0.15 mm.

Results and Discussion

The first part of the paper compares the results from experiments performed on gradients generated from relatively simple alkanethiols with those obtained from alkanethiols having more complex OEG tails. Scanning ellipsometry, XPS, and IR data are used to obtain information about the composition and appearance of the gradient profiles, as well as about the coverage and chain and tail group conformation. The second part describes the use of the gradients in experiments aiming at improving the understanding of the monolayer properties leading to low levels of nonspecific protein adsorption to organic surfaces. A sticky and often used model protein, fibrinogen, is utilized for this purpose. We describe also the use of the gradient approach for obtaining ideal

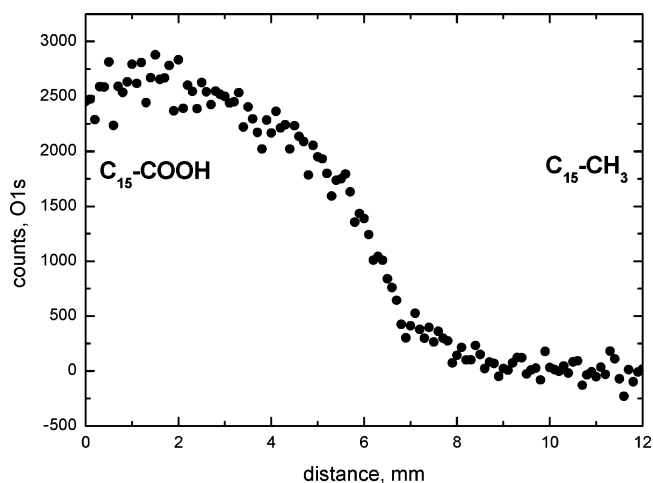


Figure 2. XPS line scan of a gradient of long-chain alkanethiols ($\text{C}_{15}\text{-COOH}$ and $\text{C}_{15}\text{-CH}_3$) prepared with the new gradient cell setup in Figure 1. The O1s peak intensity was monitored over a distance of 12 mm at a step size of 0.1 mm. The lateral resolution of the XPS setup was 0.15 mm.

Table 1. Thickness (nm) and Width (mm) of the Gradients

diffusion pair	thickness span (nm)	width (mm)
$\text{C}_{15}\text{-CH}_3/\text{C}_{15}\text{-COOH}$	1.95/2.15	5 ^a
Eg_2/Eg_6	2.7/3.8	10
Eg_4/Eg_6	3.3/3.9	7
$\text{Eg}_4/\text{Eg}_6\text{-COOH}$	3.15/4.15 ^b	>8
$\text{Eg}_6/\text{Eg}_6\text{-COOH}$	3.9/4.45	4
$\text{Eg}_2/\text{biotin-OEG}$	2.7/4.2	~ 9

^a Determined from XPS, Figure 2, because the thickness contrast was too small. ^b Broad gradient that never reached the saturation thickness on the $\text{Eg}_6\text{-COOH}$ side.

immobilization conditions of streptavidin to biotinylated surfaces. A pI gradient using $\text{C}_{15}\text{-COOH}/\text{C}_{16}\text{-NH}_2$ thiols is also described. This gradient was evaluated with respect to its ability to separate pepsin and lysozyme on a single sample surface.

Alkanethiol Gradients. The purpose of these experiments is to ensure that our novel cross-diffusion setup, Figure 1, leads to similar gradient profiles to those observed before using a slightly different setup.^{21,22} Figure 2 shows the gradient profile obtained by monitoring the O1s peak intensity of the COOH group in the XPS spectrum of a $\text{HS-(CH}_2\text{)}_{15}\text{-COOH}/\text{HS-(CH}_2\text{)}_{15}\text{-CH}_3$ ($\text{C}_{15}\text{-COOH}/\text{C}_{15}\text{-CH}_3$) gradient, using a step size of 0.1 mm. The width of the gradient regime is $\sim 4\text{-}5$ mm, a value that is in good agreement with recent results on similar systems.²² Thus, it is evident that the introduction of tracks and barriers, Figure 1, that only allow for diffusion in one direction, has a marginal effect on the appearance and width of the gradients. The advantage though of using the new setup is that smaller volumes (amounts) of thiols are required to form the gradients. Ellipsometry was also used to characterize the $\text{C}_{15}\text{-COOH}/\text{C}_{15}\text{-CH}_3$ gradient, and the thickness and width values are given in Table 1.

OEG 1D Gradients. Ellipsometry was employed as the main technique for monitoring the gradient thickness as a function of distance of the gold samples. The thicknesses obtained from the gradients at the extreme sides are in good agreement with the thicknesses observed for the corresponding single component SAMs, Table 1 and Chart 1. Increasing the OEG chain length with one ethylene glycol unit previously has been shown to give rise to an incremental increase in the SAM thickness of ~ 0.28 nm.⁴⁰ For example, the Eg_2/Eg_6 and Eg_4/Eg_6

(53) Engquist, I.; Lundström, I.; Liedberg, B. *J. Phys. Chem.* **1995**, *99*, 12257-12267.

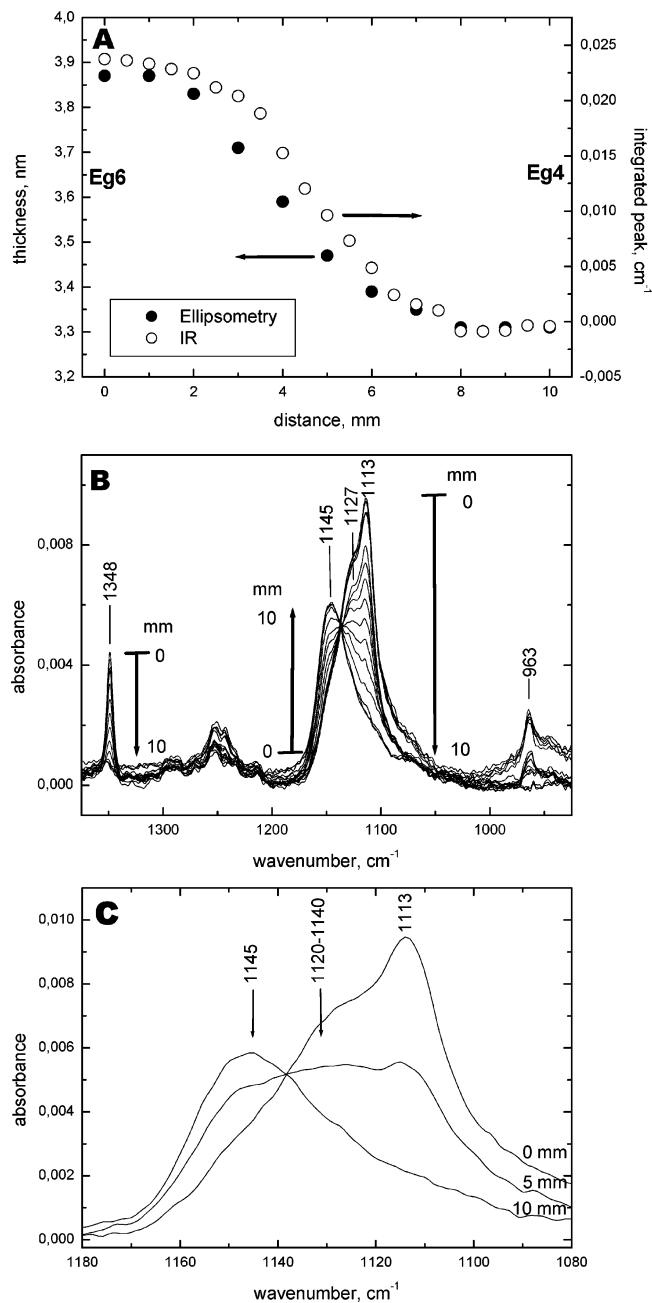


Figure 3. (A) Ellipsometry thickness, 1 mm step size, and integrated peak area, 0.5 mm step size, of the helical CH₂-wagging peak at 1348 cm⁻¹ vs distance for a Eg₄/Eg₆ gradient. (B) Stacked infrared RA spectra in the low frequency regime. In the plot are a few spectra at the extreme Eg₄/Eg₆ sides omitted to make it clearer. (C) Enlarged skeletal C–O and C–C stretching region recorded at 0, 5, and 10 mm, respectively.

gradients display thickness values between 2.7 and 3.8 nm (i.e., a difference of $\sim 4 \times 0.28$ nm) and 3.3 and 3.9 nm ($\sim 2 \times 0.28$ nm), respectively. Figure 3A shows a plot of the ellipsometric thickness (closed circles) obtained for the Eg₄/Eg₆ gradient. The gradient profile is ~ 7 mm long. The profile becomes wider (~ 10 mm) and less well defined when Eg₄ is replaced with Eg₂, a phenomenon that is attributed to the faster diffusion (shorter retention time) of the Eg₂ thiol in the Sephadex matrix. The fact that we never reach the expected 3.9 nm at the Eg₆ side of the Eg₂/Eg₆ gradient is most likely due to rapidly diffusing Eg₂ and thus to the presence of a small amount of Eg₂ in the Eg₆ assembly, Table 1. The same trend is observed for the Eg₂/OEG–biotin and Eg₄/Eg₆–COOH gradients that

are ~ 9 and > 8 mm wide, respectively. The Eg₆/Eg₆–COOH gradient profile, on the other hand, is sharper, ~ 4 mm. It seems therefore reasonable to conclude that the width of the gradient profiles increases with increasing difference in molecular complexity and retention time between the pair of molecules used in the gradient preparation procedure. This observation is not surprising considering that Sephadex LH-20 is a chromatographic material that normally is used to separate small molecules such as vitamins, steroids, lipids, and hormones.

The OEG thiols used here display a number of very interesting properties that turn them into an attractive model system for a range of applications. First of all, we as well as others^{40,42} have shown that they undergo lattice and chain length dependent phase transitions when assembled on gold and silver, respectively. Single component SAMs of Eg₂ and Eg₄, for example, assemble with the ethylene glycol portion in the all-trans conformation, whereas Eg₆ and longer ones adopt the 7/2 helical conformation.^{42,46–47,52} It is therefore of interest to investigate whether it is possible to form conformational OEG gradients with the present cross-diffusion setup. Figure 3B shows a series of stacked infrared RA spectra in the fingerprint region obtained by scanning the Eg₄/Eg₆ gradient at a step size of 0.5 mm. It is evident that the spectra vary considerably when moving along the gradient (note that a few of the spectra near the extreme sides are removed from the stacked plot in order to make it clearer). At the Eg₆ side (0 mm) is the RA spectrum characterized by a number of strong peaks at 2894 (not shown), 1348, 1113, and 963 cm⁻¹, respectively. These peaks are all typical for OEG chains in the helical conformation⁴² and confirm that the gradient assembly adopts the helical conformation on the extreme Eg₆ side. The helical peaks diminish and a new strong one appears at 1145 cm⁻¹ when moving toward the extreme Eg₄ side (10 mm). This peak is characteristic for OEG tails in the all-trans conformation.⁴² The assignments of the more prominent peaks in the spectra of the Eg₄/Eg₆ gradient as well as for the other gradients and single component SAMs are given in Table 2. A new broad and featureless peak becomes visible near 1120–1140 cm⁻¹ in the middle of the gradient, at ~ 5 mm. This broad peak has been attributed to the amorphous phase of OEG, Figure 3C. A similar type of plot as the one in Figure 3A can be obtained for the Eg₂/Eg₆ gradient. However, as mentioned before, the profile becomes in this case wider (~ 10 mm) due to the rapidly diffusing Eg₂, making it hard to identify such a clearly defined helical phase at the extreme Eg₆ side, as shown in Figure 3B and C. Nevertheless, our scanning infrared RA results clearly show that it is possible to prepare conformational gradients that display a variation in OEG chain conformation from all trans on the extreme Eg_{2,4} sides, via an amorphous-like phase in the mixing regimes, to helical at the extreme Eg₆ sides. The scanning RA spectra in Figure 3 has also been used to determine the gradient profile by plotting the integrated intensity of the 1348 cm⁻¹ peak versus distance (millimeters). This plot is shown in Figure 3A (open circles) together with ellipsometric thickness (closed circles), and we conclude that there is very good agreement between the two methods used to calculate the profile. It should be emphasized, however, that it is not always possible to utilize RA spectroscopy for obtaining reliable intensity profiles. This is due to the fact that the mode intensities in a RA spectrum are very sensitive to changes in orientation of the molecular building blocks (groups) with respect to the metal surface because of the surface dipole selection rule.⁴²

Table 2. IR Mode Assignments (cm⁻¹) of the Main Features in the OEG-Containing SAMs

mode assignment	Eg ₂	Eg ₄	Eg ₆	Eg ₆ -COOH	biotin-OEG
CH _x (biotin)					2972
alkyl, CH ₂ asym stretch, d ⁻	2918	2918	2917	2917	2918
CH ₂ , helical (OEG)			2894	2984	
CH ₂ , all trans (OEG)		2876			
alkyl, CH ₂ sym stretch, d ⁺	2850	2850	2850	2850	2850
C=O stretch (COOH)				1732	
C=O stretch (biotin)					1710
amide I (C=O)				1646	1657
amide II (C-N-H)	1562	1559	1555	1557	1556
CH ₂ scissor, bend	1463	1465	1464	1460, 1427	1467, 1432
C-O-C helical (OEG)			1348	1347	
biotin ring					1268
amide III ^a + C-O-C all trans (OEG)	1252	1252	1252	1251	
amide III ^a + C-O-C helical (OEG)			1244		
C-O-C all trans (OEG)	1141	1145			1139
C-O-C amorphous (OEG)				1120-1140 ^b	
C-O-C helical (OEG)			1113	1115	
C-OH (OEG)	1068				
C-O-C helical (OEG)			963	964	

^a The amide III (C-N-H) peak appears as a broad feature near 1250 cm⁻¹. ^b Peaks due to helical OEG (polarization perpendicular to the helical axis) also appear in this region, ref 49.

The alkyl portion contributes to two strong peaks in the RA spectra, the asymmetric (d⁻) and symmetric (d⁺) CH₂ stretching modes. Frequencies near 2917 and 2850 cm⁻¹ for d⁻ and d⁺, respectively, are characteristic for highly organized all-trans alkyl chains. The introduction of disorder in the chains forces the d⁻ and d⁺ modes to move toward higher frequencies, as can be seen upon thermal annealing of alkanethiols.^{46,47} The constant values of the d⁻ and d⁺ modes at 2917–2918 cm⁻¹ in the spectra of the OEG gradients regardless of position along the gradient confirm that alkyls adopt a densely packed all-trans conformation, Table 2. This is an improvement, as compared to our previous studies of simple alkanthiol gradients, in which the d⁻ mode was observed in the 2919–2920 cm⁻¹ region. The origin of the improvement in alkyl chain conformation is undoubtedly attributed to an additional stabilizing force introduced by the laterally interacting (hydrogen-bonding) amide groups.^{46,47}

The 1D gradients described above can be extended into more complex 2D gradients by letting four different thiols diffuse across each other along tracks 1–3 and 2–4, respectively, Figure 1. The analysis of such gradients is rather time-consuming using scanning methods and requires imaging technologies. Ongoing studies of 2D gradients using imaging methods such as surface plasmon resonance and ellipsometry will be reported on separately. We describe in the following sections the use of 1D gradients for studies of protein adsorption, separation, and immobilization phenomena.

Protein Adsorption. Poly(ethylene glycol) (PEG) and OEG modified surfaces are well-known to hinder the nonspecific adsorption of proteins. Several groups have reported on the lack of adsorption of a sticky model protein, fibrinogen, onto OEG SAM modified noble metal surfaces^{39,40,43,44} with very encouraging results. The ability to reject proteins from adsorbing on the modified surface is, however, correlated to the length, conformational properties, density, and the chemistry of the terminal group of the ethylene glycol portion, and many different models have been suggested to explain the protein rejecting properties of OEGs.^{40,48} Harder et al., for example, observed that large quantities of fibrinogen adsorbed on all-trans OEG SAMs whereas helical ones were fibrinogen rejecting.⁴⁰ Thus, gradients prepared from Eg₄/Eg₂ (all trans) and Eg₆ (helical), Figure 3, would constitute an excellent model system for protein adsorption studies, as they

provide information not only from adsorption phenomena occurring at the extreme sides but also from a broad spectrum of conformational states (amorphous-like) in the middle of the gradient. Thus, it is from a single experiment possible to obtain information from a multitude of surface-protein interaction phenomena that otherwise would require the preparation of a large number of fixed composition samples. Figure 4A shows a series of RA spectra obtained from a Eg₆/Eg₂ gradient exposed to fibrinogen, pH 6. Two methods are used to quantify the amount of nonspecifically bound fibrinogen: (I) the integrated area of the amide I peak (the arrow in part A indicates the frequency interval used to calculate the peak area) and (II) the change in ellipsometric thickness. The results are summarized in Figure 4B, and both methods agree very well. Although the Eg₆/Eg₂ gradient is slightly wider than the one obtained for the Eg₆/Eg₄ gradient in Figure 3, it is evident that the amount of bound fibrinogen increases continuously from a very low level on the Eg₆ side into a significant amount (~0.8 nm) on the Eg₂ side. Thus, *helical* OEG tails (Eg₆ side) appear to be protein rejecting, whereas the presence of conformationally disordered tails (in the mixing regime) and *all-trans* tails (Eg₂ side) seems to increase the amount of nonspecifically adsorbed fibrinogen.

A number of OEG gradients containing negatively charged tails at neutral pH were also investigated with respect to their protein adsorbing properties. Gradients of Eg₆/Eg₆-COOH and Eg₄/Eg₆-COOH were characterized before and after exposure to fibrinogen. Figure 5A illustrates the gradient (closed circles) and fibrinogen (open circles) profiles obtained with scanning ellipsometry for the Eg₆/Eg₆-COOH gradient. The gradient profile is ~4 mm wide. It is interesting to note that the fibrinogen adsorption pattern appears to be very sensitive to the composition of the SAM. Fibrinogen appears virtually nonadsorbing up to 8 mm (open circles), corresponding approximately to a COOH surface composition of 70% (estimated from the gradient profile (closed circles) as [(d_{8mm} - d_{0mm})/(d_{10mm} - d_{0mm})]100%). Fibrinogen starts to adsorb rapidly above 70% COOH, and it reaches a layer thickness of ~2 nm at 100% coverage (10 mm). Thus, the transition from nonadsorbing to adsorbing occurs over a narrow range of compositions (short distance). A similar trend is observed for the Eg₄/Eg₆-COOH gradient, Figure 5B, but the transition from nonadsorbing to adsorbing

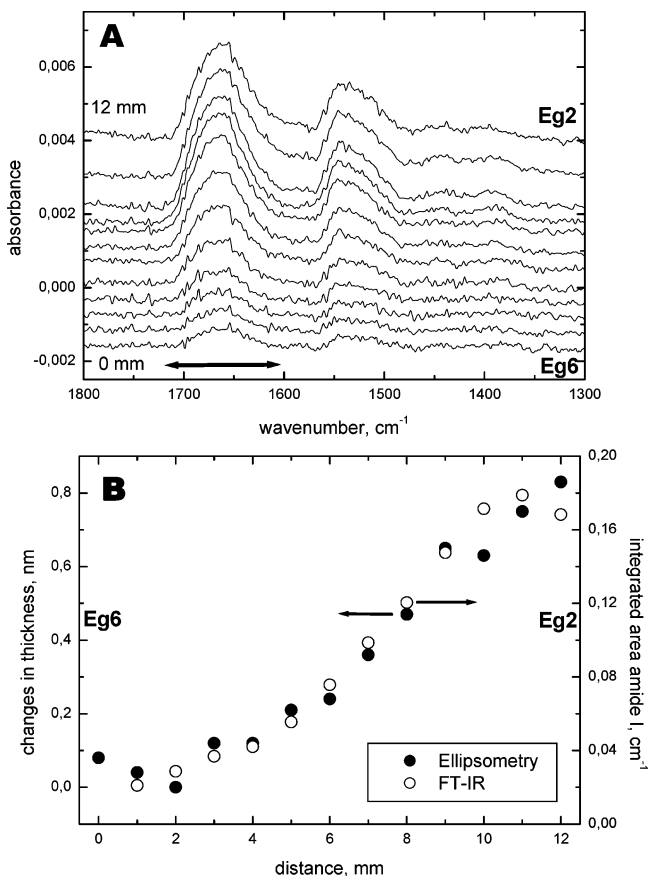


Figure 4. Adsorption of fibrinogen (pH 6, 250 $\mu\text{g}/\text{mL}$) on a Eg_2/Eg_6 gradient sample (1.5 h exposure time). (A) Stacked infrared RA spectra in the amide I and amide II region recorded at a step size of 1 mm. (B) Change in ellipsometric thickness (closed circles) and integrated area of the amide I peak (open circles) as a function of distance. The region used to calculate the integrated amide I area is marked with an arrow in part A.

occurs at a much lower composition of COOH species in the monolayer, and the fibrinogen adsorption profile seems, at least initially, to follow the gradient profile. It should also be noticed that the gradient profile is much wider for the $\text{Eg}_4/\text{Eg}_6\text{-COOH}$ gradient than for the $\text{Eg}_6/\text{Eg}_6\text{-COOH}$ gradient, and it seems that the thickness of the assembly at the extreme COOH side ($\text{Eg}_4/\text{Eg}_6\text{-COOH}$ gradient) never reaches the expected thickness of a single component $\text{Eg}_6\text{-COOH}$ SAM. This can in fact be seen if we compare the thicknesses at the $\text{Eg}_6\text{-COOH}$ sides for the two gradients. The maximum thickness seen for the $\text{Eg}_4/\text{Eg}_6\text{-COOH}$ gradient is ~ 4.1 nm, whereas the same thickness for the $\text{Eg}_6/\text{Eg}_6\text{-COOH}$ gradient is ~ 4.4 nm. Again, this is most likely due to the much faster diffusion of the Eg_4 compound. Thus, the compositions at the extreme $\text{Eg}_6\text{-COOH}$ sides of the two gradients, Figure 5A and B, are not identical, and it is therefore not surprising that the level of nonspecific protein is different for the two gradients at the $\text{Eg}_6\text{-COOH}$ side. The exact mechanism behind the increased adsorption is, however, not known. Thus, we are at present not able to provide a conclusive explanation for the difference in appearance of the two gradient profiles. However, we believe that these types of observations are of general interest in the biomaterials community, since fibrinogen, which is an important plasma protein in the coagulation cascade, is known to bind and activate platelets on charged surfaces, for example, silica, titanium, and SO_3^- and COO^-

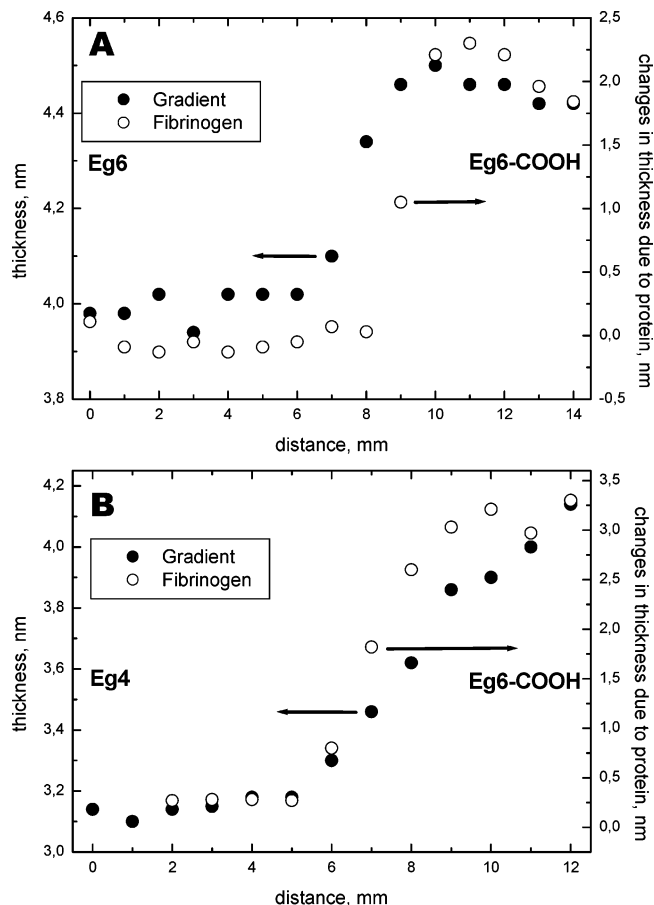


Figure 5. Ellipsometric thicknesses of the $\text{Eg}_6/\text{Eg}_6\text{-COOH}$ (A) and $\text{Eg}_4/\text{Eg}_6\text{-COOH}$ (B) gradients before (closed circles) and after (open circles) fibrinogen adsorption. The incubation time was 1.5 h, the fibrinogen concentration was 250 $\mu\text{g}/\text{mL}$, and the pH was 6.0.

terminated SAM surfaces.^{54–56} It is therefore likely that the present gradient approach can be developed into a powerful tool for identifying critical surface properties of relevance for the development of novel and improved biomaterials.

Another potential application of the alkanethiol gradients is to utilize them for surface-based separation of proteins. We have, for example, prepared a gradient in charge, a sort of pI gradient, by cross-diffusing NH_2 - and COOH -terminated thiols (e.g., $\text{C}_{15}\text{-COOH}/\text{C}_{16}\text{-NH}_2$). This gradient is fairly wide, $\sim 15\text{--}20$ mm (data not shown), and possesses positively charged NH_3^+ and negatively charged COO^- tails at neutral pH. The pI gradient is then exposed to two proteins having very different isoelectric points (lysozyme, pI ~ 10.5 ; pepsin, pI ~ 1.0), and the amount of adsorbed protein is characterized with ellipsometry. Figure 6 displays the thickness profiles obtained after exposure to pepsin and lysozyme at pH 6.0 (note the different thickness scales). It is evident that the negatively charged pepsin molecule adsorbs preferentially on the positively charged NH_3^+ side, whereas the positively charged lysozyme molecule adsorbs on the COO^- side. Although preliminary, our first set of data clearly reveals that it is possible to separate proteins with respect to the

(54) Tengvall, P.; Askendal, A.; Lundström, I.; Elwing, H. *Biomaterials* **1992**, *13*, 367–374.

(55) Lestelius, M.; Liedberg, B.; Tengvall, P. *Langmuir* **1997**, *13*, 5900–5908.

(56) Kozin, F.; Cochrane, C. G. In *Inflammation: Basic Principles and Clinical Correlates*; Gallin, J. I., Goldstein, I. M., Snydermann, R., Eds.; Raven Press, Ltd.: New York, 1988.

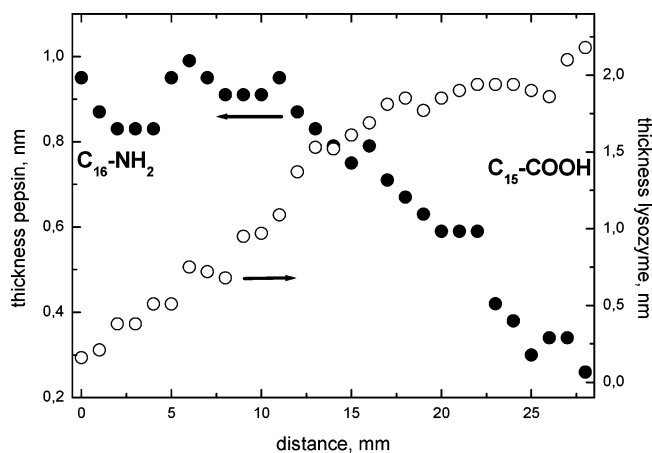


Figure 6. Adsorption of pepsin and lysozyme to a pI gradient (C₁₆-NH₃⁺/C₁₅-COO⁻) studied by scanning ellipsometry. The adsorption time was 1.5 h, the concentration was 1 mg/mL, and the pH was 6.0.

average charge using a C₁₅-COOH/C₁₆-NH₂ gradient surface. These findings in combination with the 2D gradient approach offer unique possibilities for generating test surfaces for separation purposes. For example, one can easily envision the preparation of gradients that separate with respect to charge in one direction and with respect to hydrophobicity in the other.

Optimization of Biosensing Surfaces Based on Biotin/Streptavidin. The strong and highly specific biotin/streptavidin interaction has been thoroughly used as a general platform to immobilize recognition molecules on biosensor and microarray surfaces.^{14,45} The biotin group is normally attached to the transducer substrate via a linker. This linker can be an alkyl- or OEG-containing sulfide, disulfide, or thiol^{45,57–58} for proper attachment to gold. One critical question that normally arises during the development of such a surface is *how should the biotin residues be distributed on the surface in order to obtain optimum binding streptavidin?* We have addressed this issue by generating a gradient between the biotin-OEG compound, Chart 1, and Eg₂. Figure 7A shows a series of stacked RA spectra of such a gradient. The RA spectra are composed of a number of common peaks for the two compounds at 1138 and 1556 cm⁻¹ that are due to the OEG and amide portions, Table 2, as well as two characteristic biotin peaks at 1268 and 1710 cm⁻¹ that increase in intensity with distance into the biotin side (see top spectrum of Figure 7A). The intensity of the characteristic 1710 cm⁻¹ peak, ν C=O of the biotin ring, is plotted in Figure 7B along with the layer thickness to obtain the gradient profile. Again, IR and ellipsometry give the same profile and width, ~10 mm. A series of identical gradients, of the type characterized in Figure 7B, were then prepared and subsequently immersed in a solution of streptavidin (100 μ g/mL, pH 7.4) for 1.5 h. The exposed gradients were then rinsed in buffer and Milli-Q water, blown dry in nitrogen gas, and finally scanned with IR and ellipsometry. The results from these analyses are plotted in Figure 7C, and it is evident that streptavidin binds to the gradient surface over a fairly broad range of compositions with a maximum close to 7 mm. If this value is compared with the gradient profile in Figure 7B, it becomes obvious that optimum immobilization occurs in

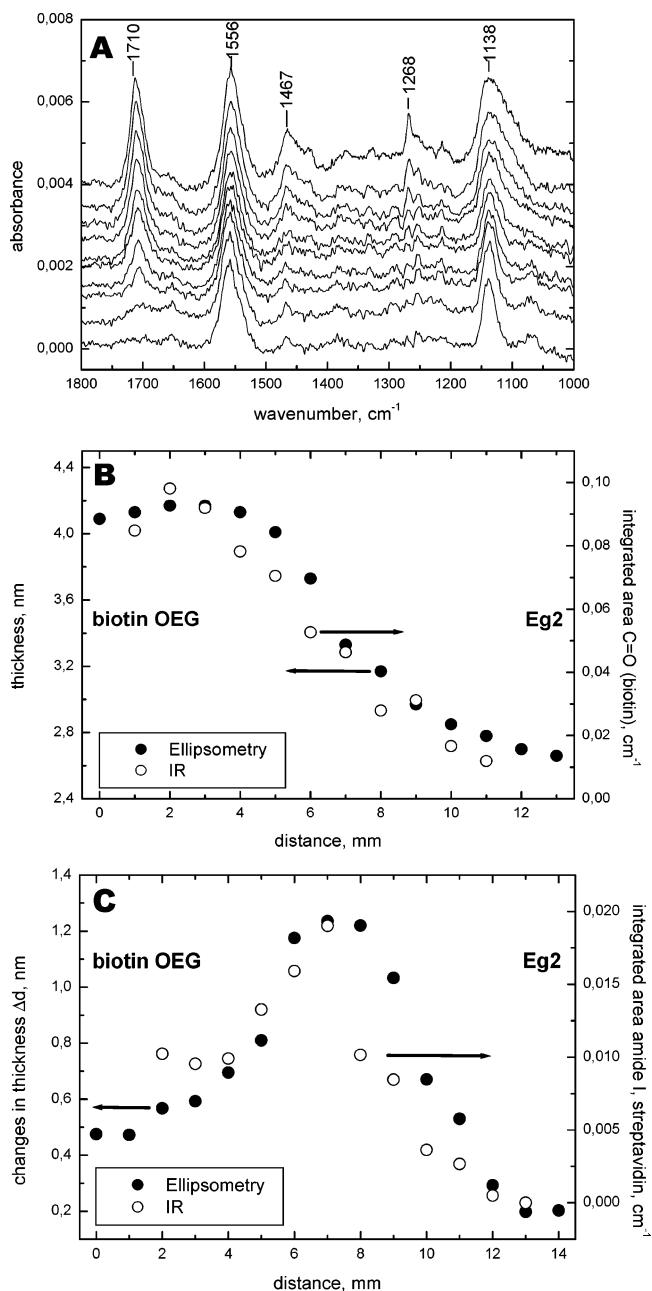


Figure 7. (A) Stacked infrared RA spectra of an Eg₂/biotin-OEG gradient in the fingerprint region (Eg₂ bottom and biotin-OEG top). (B) Ellipsometric thickness of gradient and integrated biotin (C=O, 1710 cm⁻¹) peak area (1750–1675 cm⁻¹) as a function of distance. (C) Ellipsometric thickness and integrated peak area (amide I of streptavidin) after adsorption of streptavidin (100 μ g/mL, pH 7.4, for 1.5 h).

the middle of the gradient, that is, at a biotin composition of ~50–60%. This result is somewhat different from recent results obtained for mixed monolayers of the same system.⁴⁵ Ellipsometry indicated in that particular case that the optimum streptavidin immobilization, resulting in an ~1.2 nm thick streptavidin layer, occurred near ~70% biotin in the SAM (Figure 7 in ref 40). Note, however, that the streptavidin profiles are fairly broad in both cases and that the optimum composition value obtained from the gradient experiments is close enough to yield a good starting point for subsequent optimization using, for example, single composition SAMs. Thus, we have demonstrated that the gradient approach can be used to obtain a fair estimate of the ideal immobilization conditions for a widespread model system, which can be employed to

(57) Mittler-Neher, S.; Spinke, J.; Liley, M.; Nelles, G.; Weisser, M.; Back, R.; Wenz, G.; Knoll, W. *Biosens. Bioelectron.* **1995**, *10*, 903–916.

(58) Nelson, K. E.; Gamble, L.; Jung, L. S.; Boeckl, M. S.; Naemi, E.; Gollidge, S. L.; Sasaki, T.; Castner, D. G.; Campbell, C. T.; Stayton, P. S. *Langmuir* **2001**, *17*, 2807–2816.

anchor many different biotinylated ligands to biosensing^{57,58} and microarray surfaces.¹⁴

The presented approach offers an enormous flexibility in preparing gradients by utilizing complicated ω -substituted alkanethiols. Moreover, the use of complex diffusion geometries, for example, radial, polygons, and so forth, can provide new surfaces for biomolecule interaction studies, and we are currently trying to utilize imaging technologies to monitor protein adsorption patterns on such gradient surfaces. Another possibility is to combine the gradient approach with patterning techniques to generate devices for the handling, manipulation, and guidance of biomolecules and cells.

Concluding Remarks

Molecular 1D gradients prepared from ω -substituted alkanethiols with different chain lengths and headgroups have been analyzed with scanning X-ray photoelectron and infrared spectroscopy and ellipsometry. A considerable part of the work focuses on a new type of conformational gradients based on cross-diffusion of oligo(ethylene glycol)-terminated alkanethiols. Infrared spectroscopy shows that these gradients display a continuous variation in ethylene glycol conformation from *all trans* at the short-chain Eg_2 side, via an *amorphous*-like phase in the gradient regime, to *helical* at the long-chain Eg_6 side. This type of conformational gradient has not been prepared before, and we have in a series of experiments illustrated how it can be used to monitor the amount of irreversibly bound fibrinogen as a function to OEG tail conformation. The outcome of these experiments is in excellent agreement

with recent studies on the corresponding single component SAMs, suggesting that the gradient method has a great potential for the identification of new surface properties of importance for the design and development of protein rejecting and antifouling materials.

The gradient approach also has been utilized to optimize the immobilization level of streptavidin onto biotinylated gold surfaces for biochip applications. This gradient is prepared by cross-diffusion of a biotinylated Eg_2 compound and Eg_2 , and the results show that high amounts of streptavidin are immobilized over a fairly broad range of compositions with a maximum near 50–60% of the biotinylated thiol in the gradient assembly. This finding demonstrates the power of the gradient method for rapid identification of a critical ligand composition and distribution.

A sort of pI gradient composed of alkanethiols bearing positively and negatively charged tail groups ($\text{NH}_3^+/\text{COO}^-$) also has been prepared and evaluated with respect to its ability to separate proteins. Experiments on pepsin and lysozyme look very promising, and attempts to extend the approach into 2D are currently being examined in combination with imaging optical methods and MALDI-TOF characterization.³²

Acknowledgment. This work was supported by the Swedish Research Council (VR) through the program Distributed Physics and Chemistry and by the Swedish Foundation for Strategic Research (SSF) through the Biomimetic Materials Science program.

LA048358M